Journal of the European Ceramic Society 22 (2002) 1857–1861

www.elsevier.com/locate/jeurceramsoc

Effect of Zn substitution on dielectric responses of 0.2PMT·0.8PMN ceramics

Min-Chul Chae, Nam-Kyoung Kim*

Department of Inorganic Materials Engineering, Kyungpook National University, Daegu 702-701, South Korea

Received 21 March 2001; received in revised form 11 October 2001; accepted 20 October 2001

Abstract

Phase developments and lattice parameters of a perovskite structure as well as dielectric responses in a $Pb[(Mg_{1/3}Ta_{2/3})_{0.2}(Mg_{1/3}Nb_{2/3})_{0.8}]O_3$ system with Zn substitution for Mg are reported. Perovskite developments were investigated by X-ray diffractometry, from which phase yields and lattice parameters with compositional change were determined. Weak-field dielectric constant values of the entire system ceramics were measured under low-frequency conditions. Phase transition modes reflected in the dielectric constant spectra were further analyzed closely to explore diffuseness characteristics. © 2002 Published by Elsevier Science Ltd.

Keywords: Dielectric properties; Perovskites; PMN; PMT; X-ray methods

1. Introduction

Lead magnesium niobate and lead zinc niobate, $Pb(Mg_{1/3}Nb_{2/3})O_3$ and $Pb(Zn_{1/3}Nb_{2/3})O_3$ (PMN and PZN, in short) are relaxor ferroelectric compounds of a complex-perovskite structure (rhombohedral symmetry), with disordered arrangements in the long-range structural configuration among the octahedral cation species. Lead magnesium tantalate $Pb(Mg_{1/3}Ta_{2/3})O_3$ (PMT) of a cubic symmetry is also a ferroelectric relaxor, with 6-fold sublattices of the perovskite structure arranged in a disordered manner. Maximum dielectric constants and corresponding temperatures of PMN,[1,2] PZN (single crystal),[1] and PMT[3–5] are $\varepsilon_{r,max} = 20{,}000$ ($T_{max} = -10$ to -5 °C), 22,000 (140 °C), and 8500–8700 (-88 to -85 °C), respectively. Recently, however, two to three times as high maximum values of 39,700–57,000 were reported in a flux-grown PZN crystal.[6]

Perovskite PMN and PMT can be synthesized rather easily via two-step calcination routes of a B-site precursor method,[7,8] which is conceptually more comprehensive than the well-known columbite process.[9,10] The method has been proven to be highly effective in the synthesis of monophasic complex-perovskite compositions. In contrast, any attempt to synthesize perovskite PZN by conventional calcining-mixed-oxide processes (or even by the two-step calcination routes) under atmospheric pressure resulted only in persistent formation of unwanted pyrochlore phase(s). Nevertheless, preparation of perovskite PZN powders were realized, but only under very high pressures[11,12] or via mechanochemical reaction routes,[13] whereas single-crystalline forms were grown by the aid of fluxes.[6,14]

In a previous report on a PMT–PMN system,[5] phase-pure perovskite powders could be prepared throughout the whole composition range. Maximum dielectric constants and corresponding temperatures changed continuously in the range of 8700–20,000 at -86 to -5 °C (1 kHz). Additionally, all of the compositions exhibited frequency-dependent dielectric relaxation. In the present study, 0.2PMT·0.8PMN ($\varepsilon_{r,max} = 15{,}000$, $T_{max} = -25$ °C[5]) was selected as the starting composition and Zn was partially/fully substituted for Mg, hoping that the superior dielectric characteristics of PZN (especially of higher $\varepsilon_{r,max}$, as compared with those of PMN and PMT) could be retained, although perovskite development might be sacrificed somewhat. In order to increase the perovskite formation yields and thereby to improve dielectric properties, system powders

* Corresponding author. Tel.: +82-53-950-5636; fax: +82-53-950-5645.

E-mail address: nkkim@knu.ac.kr (N.-K. Kim).

0955-2219/02/$ - see front matter © 2002 Published by Elsevier Science Ltd.
PII: S0955-2219(01)00491-5

were prepared using the B-site precursor method, which in the present study involves prereactions of MgO, ZnO, Ta_2O_5, and Nb_2O_5 to form B-site precursor compositions of $B'B''_2O_6$-type, prior to further reactions with PbO.

2. Experimental

Compositions of the Zn-substituted 0.2PMT·0.8PMN system under investigation can be expressed as $Pb[(Mg_{1-x}Zn_x)_{1/3}(Ta_{0.2}Nb_{0.8})_{2/3}]O_3$, with values of x (0.0–1.0) at regular intervals of 0.2. The raw materials used were oxide chemicals of high purity (>99.5%). In order to preclude the effects of adsorbed moisture and to maintain the stoichiometries as closely to the nominal values as possible, the moisture contents of the raw chemicals and of the precursor powders were measured and introduced into the batch calculation.

B-site precursor powders of $(Mg_{1-x}Zn_x)(Ta_{0.2}Nb_{0.8})_2O_6$ were prepared by calcining stoichiometric mixtures at 1050–1200 °C in air. After PbO addition (also in stoichiometric proportions), the powder batches were calcined at 800–850 and 800–1050 °C for 2 h each, with intermediate steps of milling and drying. Calcined powders were examined by X-ray diffractometry (XRD) to identify the phases developed. Prepared powders (with 2 wt.% polyvinyl alcohol added as binder) were isostatically formed into pellets. The preforms were densified at 1050–1250 °C for 1 h in a multiple-enclosure crucible-setup (where the samples were embedded in the identical composition powders[15]) to suppress lead volatilization at high temperatures. Major faces of the sintered pellets were ground, polished, and Au-sputtered for electrical contacts. Weak-field ($\sim$1 V_{rms}/mm) low-frequency (10^3–10^6 Hz) dielectric responses were monitored, using an impedance analyzer on cooling.

3. Results and discussion

In the XRD spectra of the B-site precursor system $(Mg_{1-x}Zn_x)(Ta_{0.2}Nb_{0.8})_2O_6$ (Fig. 1), only a columbite structure was identified throughout the whole composition range. Similarly, only columbite crystalline solutions were formed in the $(Mg,Zn)Nb_2O_6$ system,[2] whereas two different structures of trirutile and tri-αPbO_2 were detected at $MgTa_2O_6$-rich and $ZnTa_2O_6$-rich compositions in $(Mg,Zn)Ta_2O_6$,[16] respectively. Therefore, it was implied by the sole development of columbite in the present system that the 20 mol% components of $(Mg,Zn)Ta_2O_6$ had lost their own crystal structures and had been completely dissolved into the host solid solutions of columbite. Meanwhile, it was found by a careful inspection of the diffraction patterns (in terms of diffraction angles) that the unit cell dimensions of the present precursor system were reduced slightly

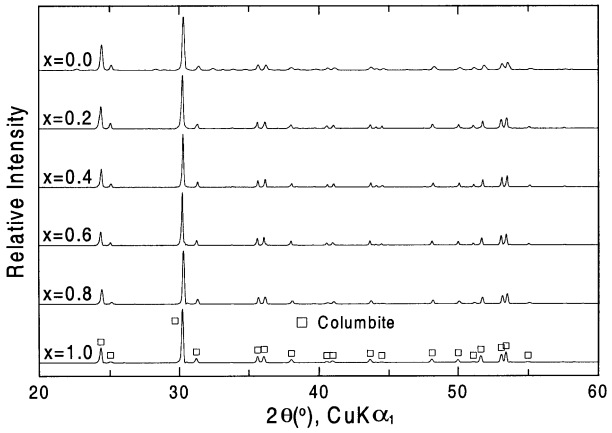

Fig. 1. X-ray diffractograms of the $(Mg_{1-x}Zn_x)(Ta_{0.2}Nb_{0.8})_2O_6$ precursor system.

from those of $(Mg,Zn)Nb_2O_6$, which is undoubtedly due to the incorporation of smaller Ta during the solid solution formation. In spite of the identical reported radii of Ta^{5+} and Nb^{5+} (0.064 nm[17]), several instances of larger lattice parameters in the Nb-containing compounds (as compared with those of Ta-analogs) are available: $Pb(Li_{1/4}B''_{3/4})O_3$,[18] $Pb(Mg_{1/3}B''_{2/3})O_3$,[5] $(Ba,Pb)(Zn_{1/3}B''_{2/3})O_3$,[19] $Pb(Fe_{1/2}B''_{1/2})O_3$,[20] $Pb(Sc_{1/2}B''_{1/2})O_3$,[20] etc.

Structures developed (after the second calcination) in the $Pb[(Mg_{1-x}Zn_x)_{1/3}(Ta_{0.2}Nb_{0.8})_{2/3}]O_3$ system are presented in Fig. 2. The pattern of $x=0.0$ (i.e. $Pb[Mg_{1/3}(Ta_{0.2}Nb_{0.8})_{2/3}]O_3$) was identified as a typical perovskite. In contrast, only a cubic pyrochlore structure (along with small amounts of PbO and ZnO) was detected at the other end of $x=1.0$ (i.e. $Pb[Zn_{1/3}(Ta_{0.2}Nb_{0.8})_{2/3}]O_3$). The two oxide components of PbO and ZnO (usually observed in the presence of pyrochlore as the major phase, e.g. $x=0.8$ and 1.0 in the present study) are believed to be by-products, left after the pyrochlore formation from powder mixtures of a perovskite stoichiometry. At intermediate compositions, perovskite was the dominant phase at $x\leqslant 0.6$, whereas pyrochlore

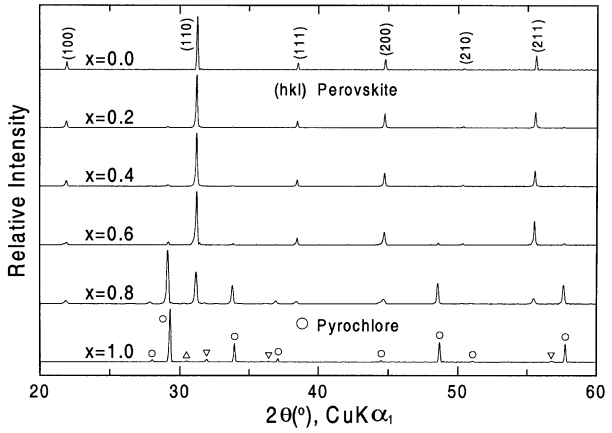

Fig. 2. X-ray diffractograms of the $Pb[(Mg_{1-x}Zn_x)_{1/3}(Ta_{0.2}Nb_{0.8})_{2/3}]O_3$ system (△: PbO; ▽: ZnO).

was higher in intensity at $x=0.8$. Meanwhile, no superlattice reflections were observable in the entire system compositions, indicating lack of long-range structural ordering among the octahedral cation species of Mg, Zn, Ta and Nb. Hence, diffuse maxima in the dielectric constant spectra are expected to develop by the local compositional inhomogeneity.

Perovskite formation yields (after sintering), determined from the XRD patterns by numerical comparison between the intensities of perovskite (110) and pyrochlore (222) reflections, are shown in Fig. 3. The values were 0% ($x=1.0$), 38% ($x=0.8$), 97% ($x=0.6$), and 100% ($x=0.4$–0.0), which increased with decreasing values of x (i.e. increasing Mg concentration) at the expense of the pyrochlore. The continuous increases can be well explained by the role of Mg with its greater ionicity and consequent favoring of the more ionic crystal structure of perovskite over the pyrochlore. Lattice parameters of the perovskite structure, based on a (pseudo)cubic symmetry, are also included in Fig. 3, where the values increased from 0.4043 nm ($x=0.0$) with increasing values of x at a rate of 0.0123 pm/at.% Zn. The gradual increase is definitely attributable to the progressive incorporation of larger Zn^{2+} (0.0740 nm[17]) in place of the octahedral Mg^{2+} (0.0720 nm[17]). Meanwhile, the parameter of $x=0.8$ was greatly deviated from the linear relation, which seems to have been influenced by the coexisting pyrochlore of greater intensity.

Temperature- and composition-dependent dielectric constant measurement results (1 kHz) are displayed in Fig. 4. The spectra at other frequencies are also included as well for $x=0.4$ only (in order to avoid a congested look), where values of the maximum dielectric constant and dielectric maximum temperature are 16,400 (15 °C), 15,400 (18 °C), 14,400 (24 °C), and 13,100 (30 °C) at 1, 10, 100, and 1000 kHz, respectively. Hence, strong dielectric dispersion (associated with diffuse modes in the phase transition) with respect to measurement frequency are well demonstrated. Other compositions of

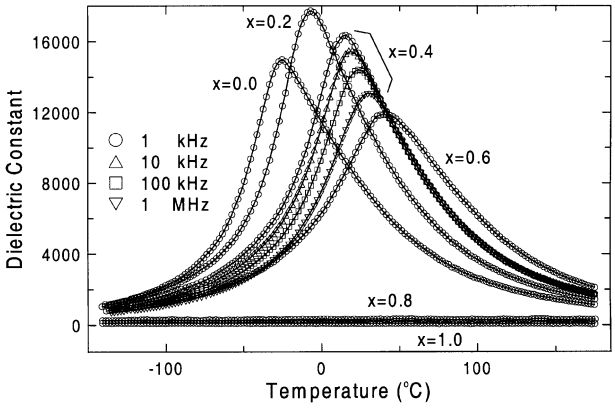

Fig. 4. Dielectric spectra of the entire system of ceramics.

$x=0.0$, 0.2, 0.6, and 0.8 also exhibited similar relaxation behavior. It should be pointed out, however, that the dielectric constant peaks at $x=0.8$ ($\varepsilon_{r,max}=310$–340 and $T_{max}=60$–70 °C, 1–1000 kHz) were so broad that they could hardly be noticed. Such low values of $\varepsilon_{r,max}$ are definitely attributable to the presence of pyrochlore (62%). In contrast, the dielectric constant values at $x=1.0$ (where perovskite yield = 0%) decreased only monotonically with increasing temperature. Room-temperature dielectric constant and temperature coefficient values were 97 and −0.15 /K, respectively.

Changes in the maximum dielectric constant and corresponding temperature of the system compositions are plotted as a function of measurement frequency in Fig. 5. As the two variables at $x=0.8$ could not be determined accurately (due to noise in the data), they are not included in Fig. 5. The dielectric maximum temperatures increased with increasing values of x (i.e. Zn concentration), regardless of frequency. In contrast, the maximum dielectric constant values reached maxima (17,700, 16,600, 15,300 and 13,800 at the four frequency decades) at $x=0.2$, followed by continuous decreases.

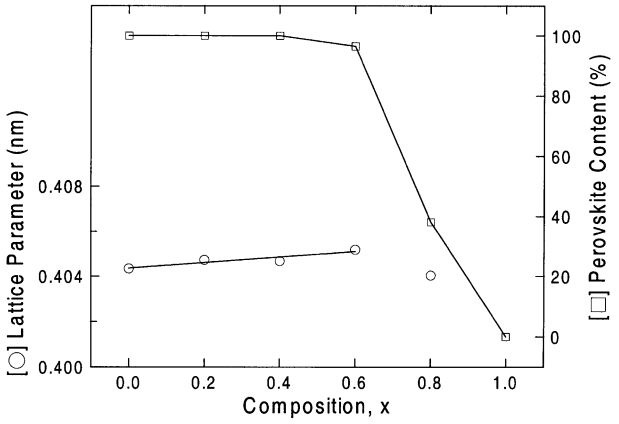

Fig. 3. Dependencies of the perovskite content and lattice parameter upon composition.

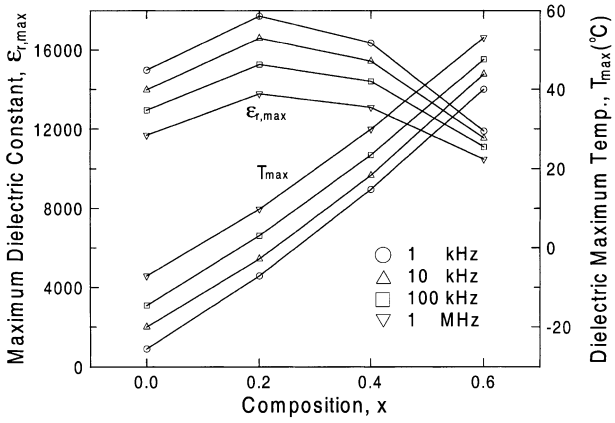

Fig. 5. Variations of the dielectric characteristics with compositional and frequency changes.

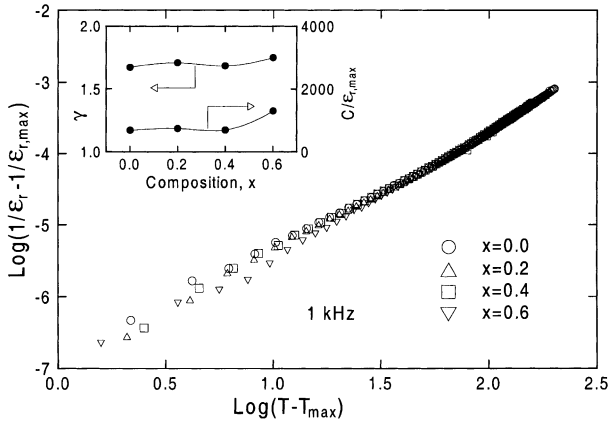

Fig. 6. $\mathrm{Log}(1/\varepsilon_r - 1/\varepsilon_{r,max})$ versus $\log(T-T_{max})$ of the system compositions. Obtained values of the diffuseness exponent (γ) and degree of diffuseness ($C/\varepsilon_{r,max}$) are plotted in the inset.

Dielectric constant spectra at the paraelectric-temperature regime are often analyzed quantitatively to explore the diffuseness characteristics of phase transition modes. Diffuseness exponent (γ) and degree of diffuseness ($C/\varepsilon_{r,max}$) are the numerical results, detailed physical meanings and derivation methods of which can be found elsewhere.[16,21–23] Fig. 6 shows dependencies of the $\log(1/\varepsilon_r - 1/\varepsilon_{r,max})$ versus $\log(T-T_{max})$ relation upon composition, with determined values of the two diffuseness parameters separately plotted in the inset. As accurate values of $\varepsilon_{r,max}$ and T_{max} of $x=0.8$ were not available, the composition was excluded in the evaluation. Whereas γ changed in the range of 1.67–1.75, the values of $C/\varepsilon_{r,max}$ were 690–1300 at the covered composition range. By referring to the two extremities of $\gamma=1$ (first-order sharp transitions in $BaTiO_3$ and $PbTiO_3$, obeying a Curie–Weiss law of $1/\varepsilon_r = 1/\varepsilon_{r,max} + (T-T_{max})/C$) and $\gamma=2$ (second-order diffuse phase transitions, obeying a quadratic law[21] of $1/\varepsilon_r = 1/\varepsilon_{r,max} + (T-T_{max})^2/C'$), the phase transitions in the present system are closer to the diffuse modes. Moreover, their variations were comparatively small, indicating relative insensitivity of the two parameters to the compositional change.

4. Summary

Continuous solid solutions of a columbite structure were developed throughout the entire composition range of the B-site precursor system. After PbO addition and calcination, in contrast, perovskite and pyrochlore structures were detected at low-to-medium and high values of x (i.e. Zn concentration). The perovskite contents increased with decreasing x and reached 100% at $\geqslant$60 at.% Mg. The lattice parameters of the perovskite structure increased steadily with increasing values of x, by the gradual replacement of Mg^{2+} by larger Zn^{2+}. Strong dispersion behavior of frequency dependence in the dielectric constant spectra was observed in all of the system compositions, except for $x=1.0$ (perovskite yield = 0%), where the dielectric constant values merely decreased in a monotonical way with increasing temperature. Whereas magnitudes of the maximum dielectric constant were highest at $x=0.2$ (e.g. 17,700, 1 kHz), the dielectric maximum temperatures increased steadily from −25 °C ($x=0.0$) to 40 °C ($x=0.6$). The hope for enhancement of $\varepsilon_{r,max}$ upon Zn substitution was not realized however. Meanwhile, the phase transition modes were analyzed to be closer to the diffuse ones, with only slight variations in the diffuseness parameters with compositional change.

Acknowledgements

This study was supported by the Korea Research Foundation Grant (KRF-99-041-E00528).

References

1. Yamashita, Y., Relaxor ceramic dielectric materials for multilayer ceramic capacitors. In *Proceedings of the Seventh IEEE International Symposium on Applications of Ferroelectrics*, 1990, pp. 241–245.
2. Chae, M.-C., Kim, N.-K., Kim, J.-J. and Cho, S.-H., Preparation of $Pb(Mg_{1/3}Nb_{2/3})O_3$–$Pb(Zn_{1/3}Nb_{2/3})O_3$ ceramics by the B-site precursor method and dielectric characteristics. *J. Mater. Sci.*, 1998, **33**(5), 1343–1348.
3. Lu, Z. G., Flicoteaux, C. and Calvarin, G., Dielectric and crystallographic study of the lead magnotantalate relaxor. *Mater. Res. Bull.*, 1996, **31**(5), 445–452.
4. Akbas, M. A. and Davies, P. K., Processing and characterization of lead magnesium tantalate ceramics. *J. Mater. Res.*, 1997, **12**(10), 2617–2622.
5. Chae, M.-C. and Kim, N.-K., Perovskite formation by B-site precursor method and dielectric characteristics of $Pb[Mg_{1/3}(Ta,Nb)_{2/3}]O_3$ Ceramic System. *Ferroelectrics*, 1998, **209**(3,4), 603–613.
6. Park, S.-E., Mulvihill, M. L., Lopath, P. D., Ziparro, M. and Shrout, T. R., Crystal growth and ferroelectric related properties of $(1-x)Pb(A_{1/3}Nb_{2/3})O_3$–$xPbTiO_3$ ($A=Zn^{2+}$, Mg^{2+}). In *Proceedings of the Tenth IEEE International Symposium on Applications of Ferroelectrics*, 1996, pp. 79–82.
7. Lee, B.-H., Kim, N.-K., Kim, J.-J. and Cho, S.-H., Perovskite formation sequence by B-site precursor method and dielectric properties of PFW–PFN ceramics. *Ferroelectrics*, 1998, **211**(1-4), 233–247.
8. Lee, B.-H., Kim, N.-K. and Park, B.-O., Perovskite formation and dielectric characteristics of $PFW_{0.2}PFT_{0.8-x}PFN_x$ system ceramics. *Ferroelectrics*, 1999, **227**(1–4), 87–96.
9. Swartz, S. L. and Shrout, T. R., Fabrication of perovskite lead magnesium niobate. *Mater. Res. Bull.*, 1982, **17**(10), 1245–1250.
10. Swartz, S. L., Shrout, T. R., Schulze, W. A. and Cross, L. E., Dielectric properties of lead magnesium niobate ceramics. *J. Am. Ceram. Soc.*, 1984, **67**(5), 311–315.
11. Matsuo, Y., Sasaki, H., Hayakawa, S., Kanamaru, F. and Koizumi, M., High-pressure synthesis of perovskite-type $Pb(Zn_{1/3}Nb_{2/3})O_3$. *J. Am. Ceram. Soc.*, 1969, **52**(9), 516–517.
12. Ravindranathan, P., Srikanth, V., Komarneni, S. and Bhalla,

A. S., Processing of $Pb(Zn_{1/3}Nb_{2/3})O_3$ ceramics at high pressures. *Ferroelectrics*, 1996, **188**(1-4), 135–141.
13. Wang, J., Wan, D., Xue, J. and Ng, W. B., Synthesizing nanocrystalline $Pb(Zn_{1/3}Nb_{2/3})O_3$ powders from mixed oxides. *J. Am. Ceram. Soc*., 1999, **82**(2), 477–479.
14. Yokomizo, Y. and Nomura, S., Dielectric and optical properties of $Pb(Zn_{1/3}Nb_{2/3})O_3$ single crystal. *J. Phys. Soc. Jpn*., 1970, **28**(Suppl.), 150–152.
15. Chae, M.-C., Kim, N.-K., Kim, J.-J. and Cho, S.-H., Preparation and dielectric properties of $Pb[(Mg_{1/3}Ta_{2/3}),(Zn_{1/3}Nb_{2/3})]O_3$ relaxor ceramics. *Ferroelectrics*, 1998, **211**(1-4), 25–39.
16. Lim, S.-M. and Kim, N.-K., Perovskite phase developments in $Pb[(Mg,Zn)_{1/3}Ta_{2/3}]O_3$ system and dielectric characteristics. *J. Mater. Sci*., 2000, **35**(17), 4373–4378.
17. Shannon, R. D., Revised effective ionic radii and systematic studies of interatomic distances in halides and chalcogenides. *Acta Cryst*., 1976, **A32**(5), 751–767.
18. Matsuoka, T., Kawashima, S., Matsuo, Y., Hayakawa, S., Ikeda, T., Nakaue, A., Inoue, K. and Yagi, Y., High-pressure synthesis of perovskites $Pb(Li_{1/4}Nb_{3/4})O_3$ and $Pb(Li_{1/4}Ta_{3/4})O_3$. *J. Am. Ceram. Soc*., 1975, **58**(7-8), 321–322.
19. Ahn, B.-Y. and Kim, N.-K., Role of B″ ion (B″ = Nb,Ta) on perovskite development, lattice parameter changes, and dielectric properties of $(Ba,Pb)(Zn_{1/3}B''_{2/3})O_3$ ceramics, submitted to J. Mater. Sci.
20. Galasso, F. and Darby, W., Preparation of single crystals of complex perovskite ferroelectric and semiconducting compounds. *Inorg. Chem*., 1965, **4**(1), 71–73.
21. Uchino, K. and Nomura, S., Critical exponents of the dielectric constants in diffused-phase-transition crystals. *Ferroelectrics Lett*., 1982, **44**(3), 55–61.
22. Butcher, S. J. and Thomas, N. W., Ferroelectricity in the system $Pb_{1-x}Ba_x(Mg_{1/3}Nb_{2/3})O_3$. *J. Phys. Chem. Solids*, 1991, **52**(4), 595–601.
23. Kuwabara, M., Takahashi, S., Goda, K., Oshima, K. and Watanabe, K., Continuity in phase transition behavior between normal and diffuse phase transitions in complex perovskite compounds. *Jpn. J. Appl. Phys*., 1992, **31**(9B), 3241–3244.